CEAS Aeronaut J
DOI 10.1007/s13272-012-0057-5

ORIGINAL PAPER

Laser-vibrometric analysis of propagation and interaction of lamb waves in CFRP-plates

J. Pohl · G. Mook

Received: 12 April 2012 / Revised: 16 November 2012 / Accepted: 13 December 2012

Abstract The use of scanning laser-vibrometry for the investigation of various phenomena of Lamb wave propagation and interaction for structural health monitoring purposes in CFRP-structures is presented. Different measuring modes and data processing are introduced to characterise piezoactuators and their wave fields, measure velocity dispersion and direction-dependent attenuation and describe the interactions with defects.

Keywords Lamb waves · Structural health monitoring · Piezoceramic actuator · Wave velocity · Wave attenuation

1 Introduction

Lamb waves offer a great potential for structural health monitoring (SHM) of thin-walled structures which are typical for lightweight design in aerospace or space industries [2, 4, 5, 7, 8, 10, 12, 21, 26]. Especially composites, e.g. carbon fibre-reinforced plastics (CFRP), are suitable for such purposes. Lamb waves, used in a structural health monitoring system, can continuously detect and further characterise different types of defects by their interactions with these defects.

J. Pohl (✉)
Hochschule Anhalt Köthen, FB Elektrotechnik, Maschinenbau und Wirtschaftsingenieurwesen, Bernburger Straße 57, 06366 Köthen, Germany
e-mail: j.pohl@emw.hs-anhalt.de

G. Mook
Otto-von-Guericke-Universität Magdeburg, Institut für Werkstoff- und Fügetechnik (IWF), Bereich Werkstofftechnik, Postfach 4120, 39016 Magdeburg, Germany
e-mail: mook@ovgu.de

However, a detailed understanding of the complex behaviour of Lamb waves in such composite plate or shell structures with regard to propagation properties and interactions with the structure and defects and of their optimal generation is necessary.

The observation of propagating Lamb wave fields by laser-vibrometry provides a non-contact detection and subsequent analysis of the different Lamb wave modes [11, 15, 25]. In this way the amplitude, velocity and attenuation behaviour as well as the interaction with defects become detectable [13, 17, 23, 24, 30]. The measurement of the vibrations of the generating piezoactuators and of the resulting wave fields helps to optimise the generation of Lamb waves for SHM-purposes.

2 Detection of vibrations and waves by laser-vibrometric measurements

Scanning laser Doppler vibrometry is a highly sensitive technology for non-contact measurement of small displacements of vibrations or wave fields. By interferometric detection, using the Doppler-effect, the vibration displacement or velocity is measured with high accuracy at each sample point. The system used for our investigations, a Polytec PSV-300 scanning laser vibrometer, determines the out-of-plane component of the surface motion. A multi-point scanning of the specimens' surface delivers the entire information of the vibration or wave field of the object. Such laser imaging methods are particularly beneficial for the visualisation, analysis and interpretation of the wave propagation effects and the wave properties.

The general arrangement for the experimental work is given in Fig. 1. A piezoceramic transducer (piezoactuator) is attached to the plate-like object and acts as an actuator

Published online: 11 January 2013

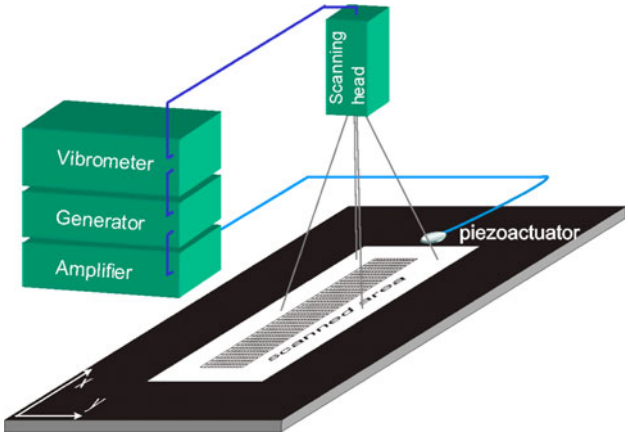

Fig. 1 Experimental arrangement for Lamb wave sensing with a scanning laser vibrometer

for Lamb wave generation. Here, different circular discs from PI Ceramics and Marco, made from different lead zirconate titanate materials (PIC 151, PIC 181, FPM 100 and FPM 202), are used as piezoceramic actuators. The diameters range from 10 to 40 mm, the thicknesses from 0.2 to 2 mm.

To provide a permanent but reversible coupling, paraffine is used as a bonding medium. The piezoactuator is driven by an electrical signal produced and amplified by a generator and an amplifier, respectively. The Lamb waves generated in this way are sensed by the laser beam emitted from the scanning head of the vibrometer system. The scanned area is formed by an appropriate grid of measuring points.

The interferometric measurement requires an adequate amount of backscattered laser light provided by a sufficient reflectivity of the specimens' surface. To ensure a sufficient intensity of back-scattered laser light from the surface of the object even in the case of the mirror-like reflecting surface of CFRP, a thin retroreflective foil or a surface whitened with the developer powder of a penetrant dye testing system was used.

The scanning laser vibrometer is a powerful tool for wave detection and analysis by offering different possibilities for data acquisition and evaluation. An excitation of the wave source with broadband chirp signals and an internal evaluation in the frequency domain by Fourier transformation give a spatial overview of the wave field in (following the terminology of non-destructive testing) C-scans for different frequencies as well as the spectral distribution at the measuring points. Unfortunately, due to the multimodal properties of Lamb waves, resulting in at least two different propagating wave modes at every frequency, such results are always a superposition of the existing modes. This is clearly seen in the C-scan of Fig. 2a, displaying both the basic symmetric mode S_0 and the basic antisymmetric mode A_0 which are identifiable by their different wave lengths. A subsequent external processing of the data allows a differentiation of the modes by spatial filtering as seen in Fig. 2b, c, displaying C-scans and spectra, respectively. In this way, the amplitude behaviour or attenuation of the wave modes can be evaluated individually.

For the determination of dispersion curves, the data have to be processed in another way. Figure 3a shows the starting point for the processing with C-scans, picked up for a broad frequency region. To cover a broad frequency range and different modes, the scanning area has to be large enough for high wavelengths on one hand, and the spatial resolution has to be fine enough to resolve small wavelengths on the other. The range of wavelengths can span from a few millimetres to more than half a metre for typical frequencies between 10 and 500 kHz in CFRP-materials. A (second) Fourier transformation of the spatial wave field provides a dispersion diagram of the wave number k over frequency, shown in the middle section of Fig. 3. For transient signals, (commonly burst signals are used) this method of applying a double Fourier transformation is described by Alleyne et al. [1], Köhler [11] and Li et al. [14]. The results only hold true for the case of plane wave fields. Deviations of wave directions (e.g. occurring in anisotropic media) manifest themselves as spurious lines in the dispersion diagram. Signal processing of the k-dispersion data with a least square routine and an adaptive curve following routine helps to filter the desired dispersion curves. Finally, the k-dispersion is converted to the presentation format velocity versus frequency, usually used for dispersion curves, as displayed in Fig. 3c.

Another measuring mode of the scanning laser vibrometer uses transient signals (e.g. bursts) for excitation and the results are displayed and evaluated in the time domain. Figure 4 gives an example of such results with an amplitude-time representation at a measuring point (A-scan) and a spatial amplitude distribution (C-Scan) for the wave propagation in a 3-mm thick plate of polymethylmethacrylate (PMMA) with a 20-mm borehole at 200 kHz. Both fundamental mode signals are visible in the A-scan as well as the C-scan image, the leading fast S_0-burst signal being followed by the slower A_0-signal.

3 Characterisation of piezoactuators and their wave fields

Piezoceramic transducers in form of small and thin piezoceramic plates are widely used for the generation of Lamb waves due to their ability of generating and receiving elastic waves, their low costs and their availability [3, 4, 7, 16, 18, 26]. Embedded or surface attached piezoactuators

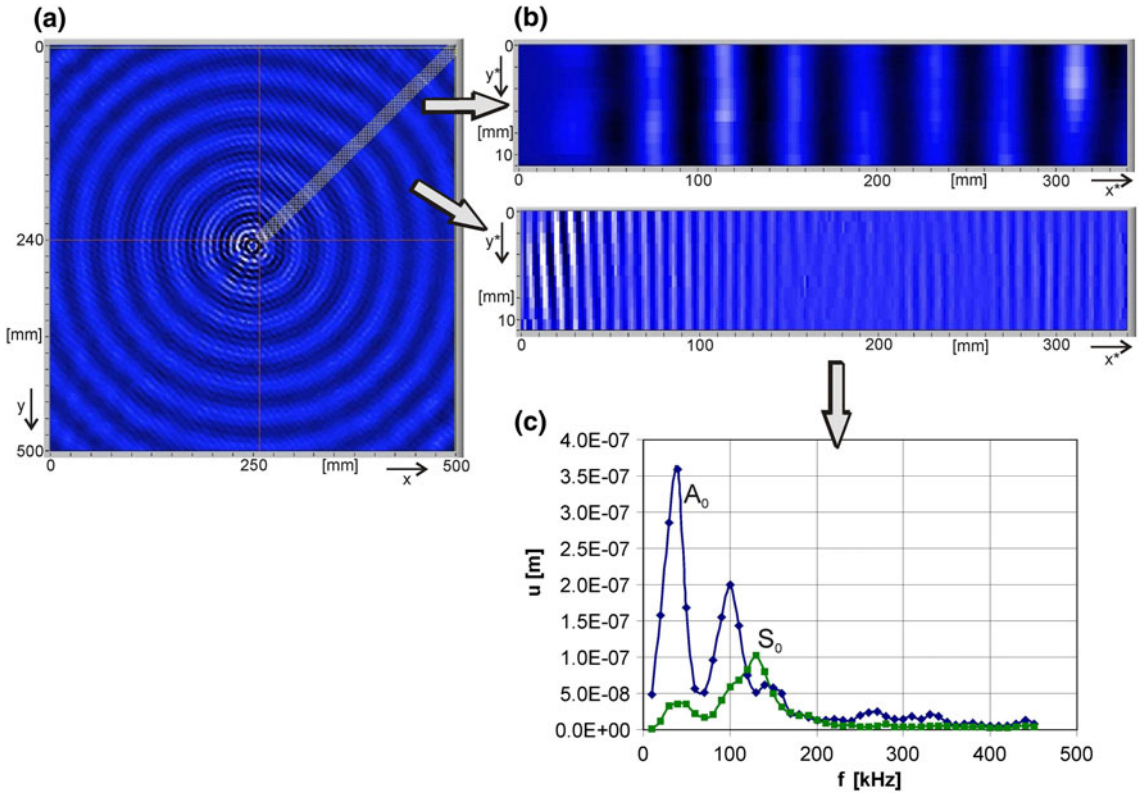

Fig. 2 **a** C-scan of A_0 and S_0 (raw data), **b** filtered data in the evaluation grid of the C-scan, displaying A_0 and S_0 separately, **c** mean spectra of A_0 and S_0 (spatial average)

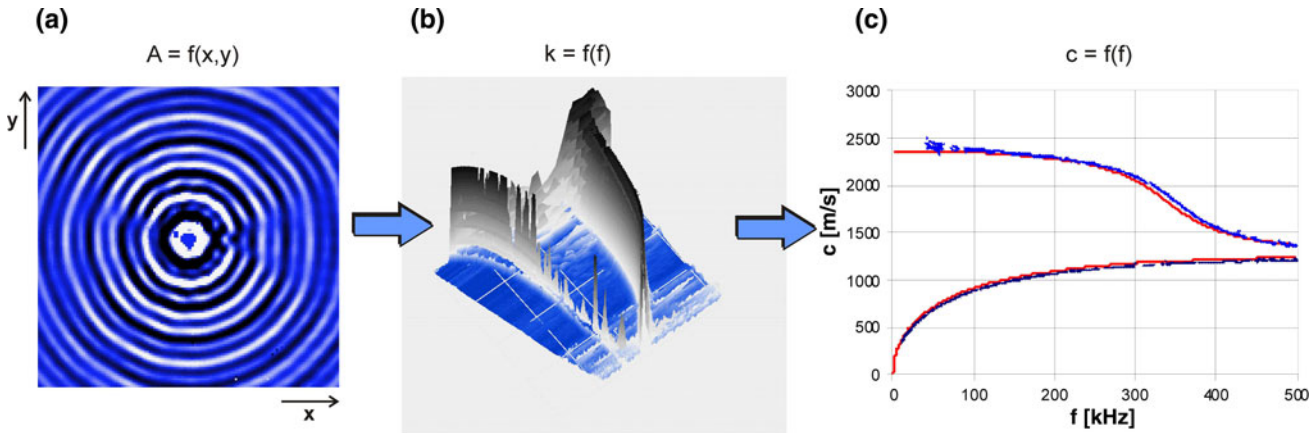

Fig. 3 Data processing for dispersion curves

generate elastic waves by coupling their vibrations to the adherent structure. The generation process of Lamb waves is thus determined by the vibration characteristics of the piezoactuator. In detail, the bending and radial modes of a bonded piezoactuator control the generation of A_0 and S_0 in the lower frequency range. The distinct modes of vibration are responsible for the strength of generation of the wave modes with their corresponding wave fields.

Scanning laser-vibrometry allows for the characterisation of the vibration behaviour by detection of the spectra and mode shapes of oscillating piezoelements. Mode shapes of different types of vibration modes are easily representable. Figure 5 presents examples of free vibrations of a circular piezoactuator (diameter 40 mm, thickness 0.5 mm, material PIC 151 from PI Ceramics). To ensure free vibrations, it was positioned free without any

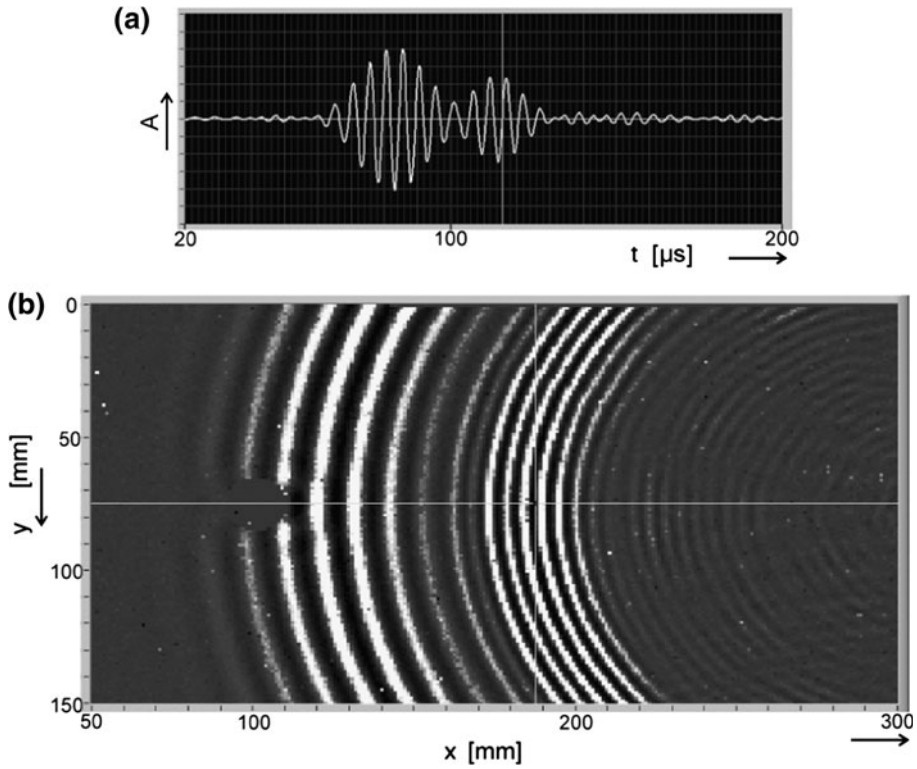

Fig. 4 Time-domain processing of vibrometer data: **a** A-scan and **b** C-scan

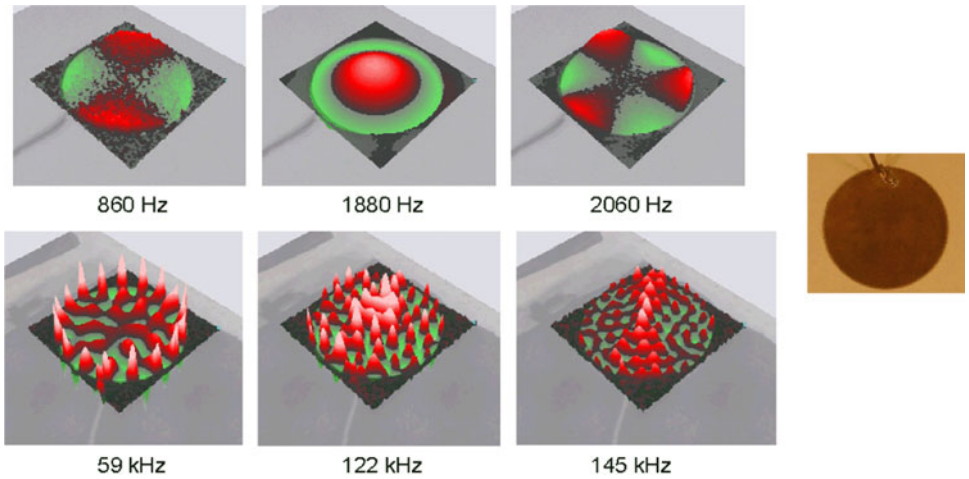

Fig. 5 Mode shapes of free vibrations of a circular piezo-actuator (diameter 40 mm, thickness 0.5 mm, material PIC 151 from PI Ceramics)

fixture. Beside the typical first three fundamental out-of-plane modes in the low frequency range, higher modes with complex and asymmetric vibration patterns are shown at higher frequencies. Even radial vibration modes with mainly in-plane displacements became detectable by their out-of-plane components of displacement produced by coupling effects.

The properties of the vibrating piezoactuators are affected by details of the design of the transducer. For example, influences of soldered contacts on mode shapes and spectra have been theoretically and experimentally observed [19, 29].

The vibration modes of the piezoactuator have consequences for the wave field formation. Huang et al. [9] reported the control of the activated Lamb wave field by the mode shape of the piezoactuator. Figure 6 gives an example for this for a circular piezoactuator, bonded to an isotropic material (PMMA). Here, a distinct mode shape with anisotropic displacement distribution produces a corresponding radiation pattern of the wave field. Because of the frequency dependence of the amplitude and the mode shapes, this effect is strongly frequency-controlled.

Another important factor is represented by the coupling of the piezoactuator to the structure by the bonding layer.

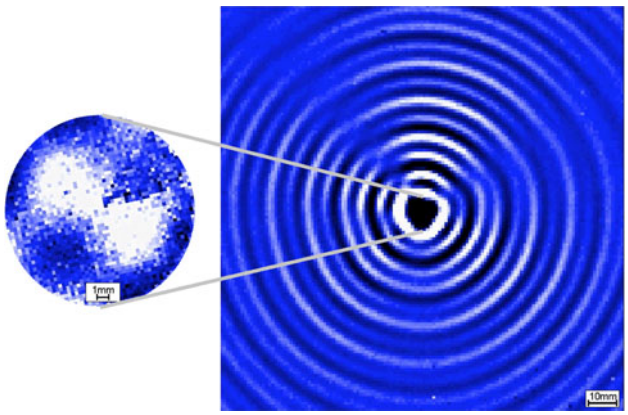

Fig. 6 Mode shape and Lamb wave field of a piezoactuator (diameter 15 mm, thickness 2 mm, material FPM 202), bonded to a PMMA-plate of 3 mm thickness at 157 kHz

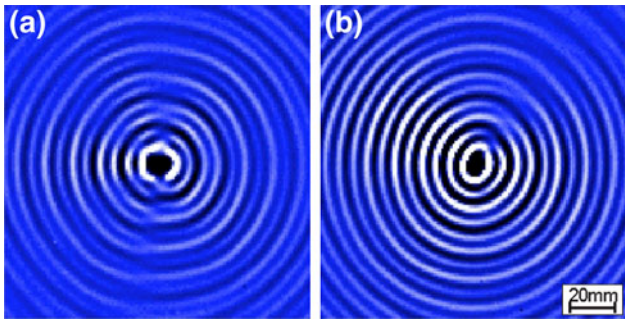

Fig. 7 Lamb wave fields of a piezoactuator (diameter 15 mm, thickness 2 mm, material FPM 202), bonded to a PMMA-plate with different coupling thicknesses **a** 2–36 µm, **b** 20–110 µm, excited at 157 kHz

Directionality and strength of wave field generation also depend on the bonding thickness and uniformity. This is validated by the results presented in Fig. 7. Here, strong directional effects due to different thickness and non-uniformity of the coupling layer affect the resulting wave fields remarkable.

The significant influence of the bonding on the vibrations of a piezoactuator is indicated in Fig. 8. Here, a polystyrene (PS) plate with 4.75-mm thickness was chosen as an isotropic medium. To compare the free and the bonded case, the corresponding mode shapes and spectra were recorded. The bonding generally results in significantly decreased amplitudes. The frequencies of resonant vibrations shift to higher values and many peaks in the spectrum are extinguished. Mode shapes in the bonded state often are only identifiable by their typical areal amplitude distribution but not in every case by a distinct peak in the spectrum.

The directionality of the Lamb wave field is not only a matter of the vibration pattern of the piezoactuator and its coupling, but also affected by anisotropic material

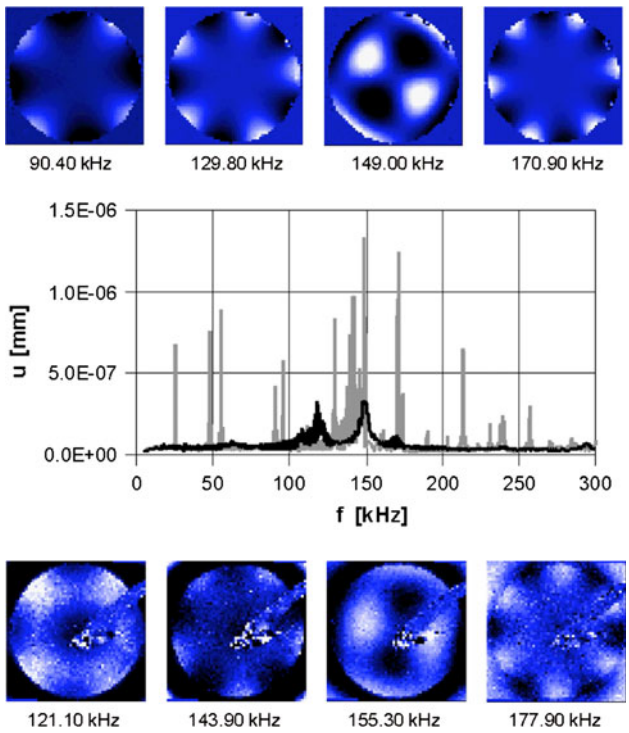

Fig. 8 Spectra (*grey* free, *black* bonded) and mode shapes (free *top*, bonded *bottom*) of a piezoceramic disc (diameter 16 mm, thickness 2 mm, PIC 181) bonded to a PS-plate

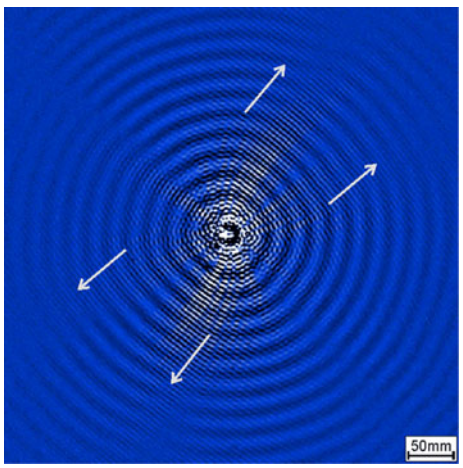

Fig. 9 Lamb wave field of a piezoactuator (diameter 10 mm, thickness 0.2 mm) at 250 kHz in a quasiisotropic CFRP-plate

properties in the case of CFRP. Even in the case of a macroscopically quasiisotropic designed CFRP material with a layup of layers with different fibre directions, the strong anisotropy of the single layer shows its influence. This is demonstrated in the case of Lamb wave propagation in a quasiisotropic plate of CFRP with a $\left[(0/90)_f/+45/-45/(\overline{0/90})_f\right]_s$ layup and a thickness of 2 mm. The C-scan in Fig. 9 displays both fundamental modes, but only A_0, indicated by its smaller wavelength,

exhibits typical anisotropy effects. Patterns of deviations of phase directions from the directions of wave propagation, marked by arrows, and bending of energy transport directions are indicators for this. The wave phase directions show differences of about 5° to the ±45°-fibre directions for this frequency. Obviously, there is a need for further research.

To sum up, experimental detection of vibrations and Lamb wave fields by scanning laser-vibrometry is a powerful tool for verification of modelling and simulation of the generation and propagation of these waves, representing an intensively studied field of research [6, 7, 22, 25, 27, 28, 31].

4 Measurement of velocity and attenuation of Lamb waves

Wave velocity as well as attenuation of Lamb waves are of basic importance for the design of a SHM-system. Knowledge of velocity is important for the differentiation of the different wave modes. For transient signals, a frequency region with low dispersion has to be chosen to prevent additional attenuation. The exact velocity is especially needed for the localisation of defects by time-of-flight evaluation of the Lamb wave signals. Because Lamb waves are always dispersive, with regions of high rate of velocity change with frequency, the special frequency dependence must be known before application. Attenuation is a limiting factor for the possible range of propagation and therefore sets limits to the maximum distances between actuators and sensors.

With the above described processing, vibrometer data are evaluated for different CFRP-plates. In addition to thinner plates with the above-mentioned $\left[(0/90)_f/+45/-45/\overline{(0/90)}_f\right]_s$ layup, a plate with 4-mm thickness and a $[(\pm 45)_f/90/-45/0/-45/90/45]_s$ layup was used. Figure 10 shows the dispersion curves of the two quasiisotropic CFRP-plates. The first three modes become resolvable in this region of frequency-thickness product. The basic antisymmetric modes show a remarkable similarity for the two different plates, but the basic symmetric and the first antisymmetric modes do not coincide in such manner. Other examples of measured dispersion curves are given in [20].

The attenuation was measured with spatial filtered broadband vibrometer data for different directions of the plate with the $\left[(0/90)_f/+45/-45/\overline{(0/90)}_f\right]_s$ layup. In this way it was possible to resolve the frequency-dependence of the attenuation coefficients for both fundamental modes, shown in Figs. 11 and 12 for the 180° direction.

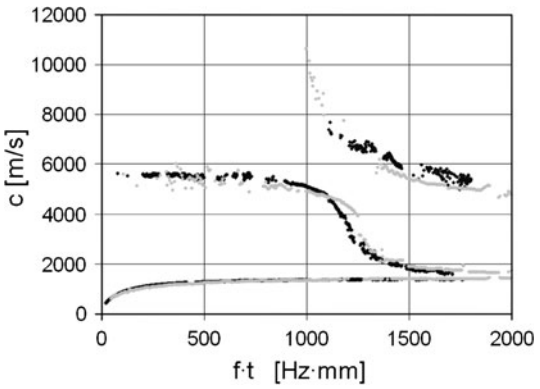

Fig. 10 Dispersion curves of the first three modes in two quasiisotropic CFRP plates (*grey* $t = 4$ mm, *black* $t = 2$ mm)

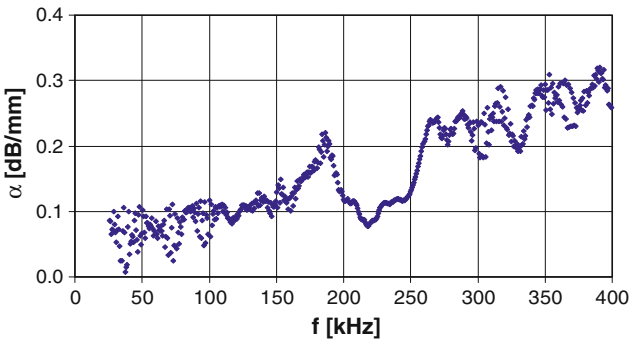

Fig. 11 Attenuation coefficients of A_0 in a quasiisotropic CFRP plate in 180° direction

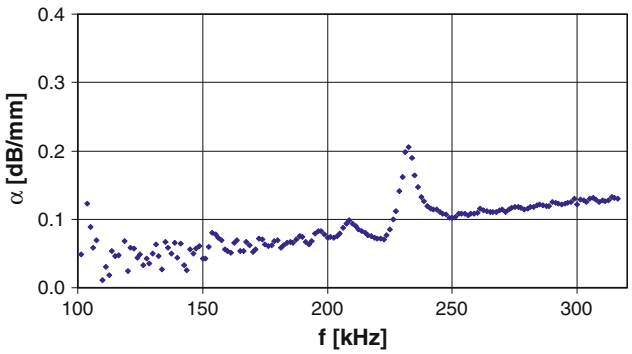

Fig. 12 Attenuation coefficients of S_0 in a quasiisotropic CFRP plate in 180° direction

The displayed attenuations represent the total attenuation, composed mainly of the material damping, the divergence of the sound field [ideally expressed by a 1/sqr(x) law] and the dispersion effect of transient signals.

As expected, the attenuation of the antisymmetric mode is considerably higher, compared to the symmetric one. A pronounced deviation from the nearly linear frequency-dependence occurs between 200 and 250 kHz.

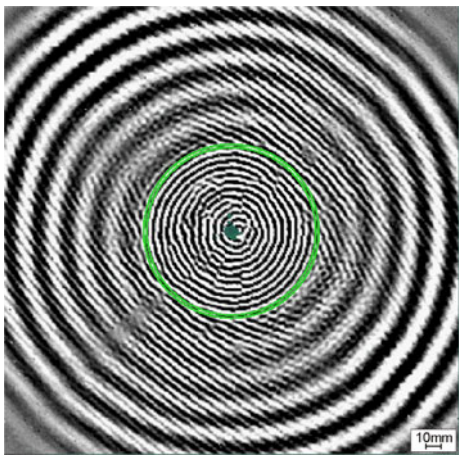

Fig. 13 C-scan in time domain, showing permanent mode conversion of S_0 into A_0 in a quasiisotropic CFRP-plate at 300 kHz

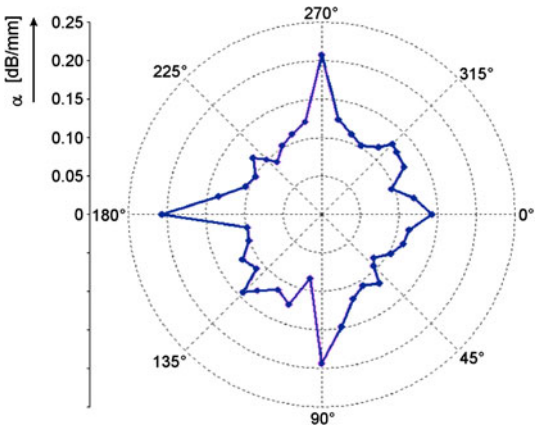

Fig. 14 Angular dependence of S_0-attenuation for 234 kHz in a quasiisotropic CFRP plate

The attenuation of S_0 sharply increases and, astonishingly, the attenuation of A_0 decreases. This behaviour can be explained by considering the evaluation of these values more precisely. Since the amplitude of the whole sound field contributes to the laser-vibrometric measured amplitudes, mode conversion effects are involved. The effect becomes visible in a presentation of the C-scan in the time domain in Fig. 13, showing permanent mode conversion of S_0 into A_0 in the quasiisotropic CFRP-plate. For better clearness, the leading front of the slower primary A_0 mode, directly launched by the piezoactuator, is marked by a circle in Fig. 13. The leading front of the faster S_0 mode is permanently superimposed by a directly following A_0 wave field, indicating the mode conversion. In this way the additional attenuation of S_0 and the amplitude increment of A_0, leading to lower measured attenuation values, is explained. In addition, the anisotropy effect of phase orientation deviation, described in Fig. 9 above, can clearly be seen in the time presentation, as well.

The mode conversion obviously mainly occurs at the oblique directed layers—here the internal ±45°-fibre directions. This is confirmed by a measurement of the directional dependence of the S_0-attenuation in the CFRP plate, shown in Fig. 14. Especially directions with maximal deviation to the 45°-directions provide maxima of attenuation, except for the 0° direction which shows, for no clear reasons, no strong attenuation.

5 Interaction with reflectors

The different interactions of Lamb waves offer possibilities for defect detection and characterisation. In addition to reflexion and transmission, mode conversion effects are of special interest for this purpose. Laser-vibrometric investigations with broadband signals and at a single frequency in the time domain are helpfully to diagnose and interpret these interactions. Tests with model reflectors help to reveal the principal reactions with defects.

Figure 15 gives an example for wave interactions with a borehole with 20-mm diameter in a quasiisotropic CFRP-plate. The piezoactuator was positioned at the right-hand corner of the image and was excited by a broadband chirp signal. The image represents a root mean square (RMS)

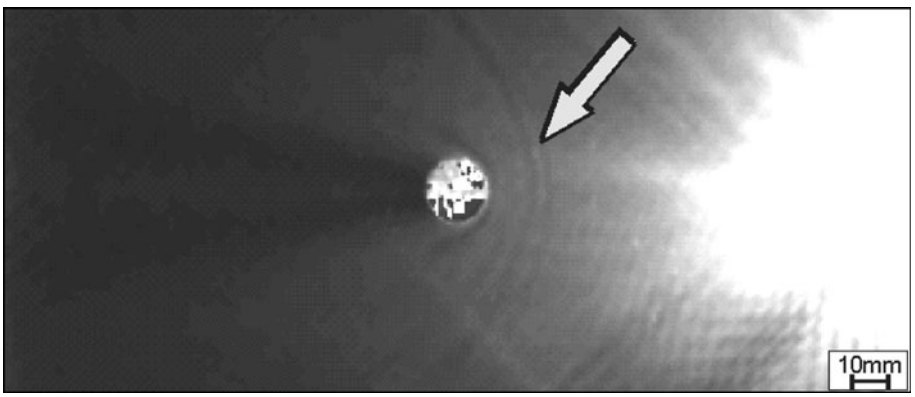

Fig. 15 Reflection and transmission of Lamb waves at a hole with 20 mm diameter with root mean square (RMS) presentation over all frequencies. The *arrow* indicates reflected A_0-waves

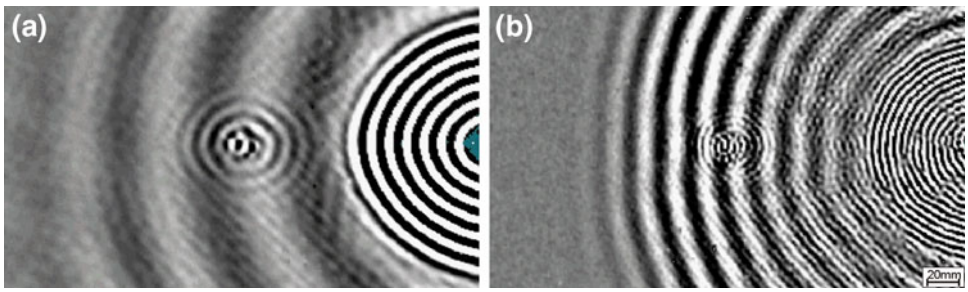

Fig. 16 Reflection with mode conversion of the S_0 mode at a *flat bottom hole* with 20 mm diameter at **a** 100 kHz and **b** 200 kHz

amplitude distribution over all frequencies and thus allows to reveal typical interactions which can be further investigated at the respective frequency in the time domain. Here, in addition to the shadowing effect of the defect with diffraction patterns, a reflection of the A_0 mode is clearly identified (arrow).

Examples for a more detailed investigation in the time domain are given in Fig. 16. The defect is represented by a flat bottom hole with 20-mm diameter and a depth of half plate thickness in a quasiisotropic CFRP-plate with 2-mm thickness. The Lamb waves are produced by a bandpass-filtered 3-cycle sinusoidal burst signal at different frequencies. The images are taken at a propagation time beyond the reflection of the impinging S_0 mode which is not displayed here. Clearly, at both frequencies a mode conversion of the S_0 mode into the A_0 mode at the defect becomes visible. In contrast to the directly reflected S_0 field, a remarkably circular field of this mode converted reflected wave developed with considerably high amplitudes even in the propagation direction of the primary S_0 wave. Such effects offer possibilities to detect, locate and characterise such types of defects with a network of distributed sensors that receive the signals from different directions.

6 Conclusions

Scanning laser-vibrometer data and its processing can contribute very beneficially to the clarification of various phenomena in Lamb wave propagation and interaction for structural health monitoring purposes. The non-contact detection of vibrations and wave fields helps to characterise the action of piezoactuators in generating the wave fields. Especially, the influence of the coupling of the transducer to the structure on the wave generation has to be clarified in more detail in future work.

The basic Lamb wave velocity and attenuation properties can be measured in their frequency and directional dependences. In addition to the directionality of the piezoactuator, these are highly important features for the design of a sensor-actuator network. Anisotropy effects occur obviously in even quasiisotropic CFRP-structures. Such effects have to be investigated for different types of CFRP-materials including effects of structural anisotropy, e.g. due to stiffening elements or thickness variations.

Finally, the detection of reflected, transmitted and mode converted Lamb waves helps to explain the complex interaction with reflectors. In this way, it is possible to optimise the choice of wave modes and frequencies for optimal detection and characterisation of typical defects.

Acknowledgments The authors like to thank the German Research Foundation (DFG) and all partners for their support (Grant number MO 553/9-1).

References

1. Alleyne, D., Cawley, P.: A two-dimensional Fourier transform method for the measurement of propagating multimode signals. J. Acoust. Soc. Am. **89**(3), 1159–1168 (1991)
2. Boller, C., Chang, F.-K., Fujino, Y.: Encyclopedia of Structural Health Monitoring. Wiley & Sons, Chichester (2009)
3. Boller, C., Biemanns, C., Staszewski, W.J., Worden, K., Tomlinson, G.R.: Structural damage monitoring based on an actuator-sensor system. In: SPIE, vol. 3668. Smart Structures and Integrated Systems, pp. 285–294. (1999)
4. Chang, F.-K.: Composite structures with built-in diagnostic. In: ICCM12, Paris, paper 799 (1999). http://www.iccm-central.org/Proceedings/ICCM12proceedings/site/papers/pap799.pdf Accessed 17 Feb 2012
5. Clarke, T., Cawley, P.: Monitoring of complex structures using guided waves. In: Proceedings of the Fourth European Workshop on Structural Health Monitoring held at Krakow, Poland July 2–4, pp. 672–679. (2008)
6. Fritzen, C.-P., Schulte, R.T.: Modelling of wave propgation and impedance spectra with the spectral element method. In: The 7th International Workshop on Structural Health Monitoring, pp. 2282–2289. DEStech Publications, Lancaster (2009). ISBN: 978-1-60595-007-5
7. Giurgiutiu, V.: Structural health monitoring with piezoelectric wafer active sensors. Academic Press, London (2008)
8. Hillger, W.; Pfeiffer, U.: Structural health monitoring using Lamb waves. In: 9th European NDT Conference, ECNDT 2006. Berlin, CD-ROM, paper Th 1.7.2 (2006)
9. Huang, H., Pamphile, T., Derriso, M.: The effect of actuator bending on Lamb wave displacement fields generated by a piezoelectric patch. Smart Mater. Struct. **17**, 1–13 (2008)
10. Kessler, S.S., Spearing, S.M., Soutis, C.: Damage detection in composite materials using Lamb wave methods. Smart Mater. Struct. **11**(2), 269–278 (2002)

11. Köhler, B.: Dispersion relations in plate structures studied with a scanning laser vibrometer. In: 9th European NDT Conference, ECNDT 2006, Berlin, paper Mo.2.1.4. (2006)
12. Kudela, P., Ostachowicz, W.: Lamb-wave based damage detection in composite structures: potentials and limitations. In: Uhl, T., Ostachowicz, W., Holnicki-Szulc, J. (eds.) Proceedings of the 4th European Workshop on Structural Health Monitoring 2008, pp. 488–495. DEStech Publications, Lancaster, Cracow, July 2–4 (2008)
13. Lammering, R.: Observation of piezoelectrically induced Lamb wave propagation in thin plates by use of speckle interferometry. Exp. Mech. **50**(3), 377–387 (2010)
14. Li, J., Liu, S.: The application of time-frequency transform in mode identification of Lamb waves. In: 17th World Conference on Nondestructive Testing, 25–28 Oct, Shanghai, China. (2008)
15. Malinowski, P., Wandowski, T., Kudela, P., Ostachowicz, W.: Laser vibrometry for guided wave propagation phenomena visualisation and damage detection. In: Tomasini, E.P. (ed.) AIP Conference Proceedings of 2010, vol. 1253. 9th International Conference on Vibration Measurements by Laser and Non-Contact Techniques, Ancona, pp. 140–149. (2010)
16. Moulin, E., Assaad, J., Delebarre, C., Kaczmarek, H., Balageas, D.: Piezoelectric transducer embedded in a composite plate: application to Lamb wave generation. J. Appl. Phys. **82**(5), 2049–2055 (1997)
17. Nadella, K.S., Cesnik, C.E.S., Salas, K.I.: Characterization of guided-wave attenuation in composite plates. In: Fifth European Workshop on Structural Health Monitoring, pp. 1205–1210. DEStech Publications, Lancaster (2010)
18. Osmont, D., Dupont, M., Lemistre, M., Gouyon, R., Kaczmarek, H., Balageas, D.: Piezoelectric based health monitoring systems for composite plates. In: Ohayon, R., Bernadou, M. (eds.) 10th International Conference on Adaptive Structures and Technologies (ICAST'99), pp. 601–608. Technomic Publication, Lancaster (1999)
19. Pohl, J., Mook, G., Lammering, R., von Ende, S.: Laser-vibrometric measurement of oscillating piezoelectric actuators and of Lamb waves in CFRP plates for structural health monitoring. In: AIP Conference Proceedings of 2010, vol. 1253. 9th International Conference on Vibration Measurements by Laser and Non-Contact Techniques Ancona, pp. 65–72. (2010)
20. Pohl, J., Szewieczek, A., Hillger, W., Mook, G., Schmidt, D.: Determination of Lamb wave dispersion data for SHM. In: 5th European Workshop on Structural Health Monitoring, pp 931–936. DEStech Publications, Lancaster (2010)
21. Raghavan, A., Cesnik, C.E.S.: Review of guided-wave structural health monitoring. Shock Vib. Dig. **39**, 91–114 (2007)
22. Salas, K.I., Nadella, K.S., Cesnik, C.E.S.: Characterization of guided wave excitation and propagation in composite plates. In: The 7th International Workshop on Structural Health Monitoring, pp. 651–658. DEStech Publications, Lancaster (2009)
23. Schubert, L., Lieske, U., Köhler, B., Frankenstein, B.: Interaction of Lamb waves with impact damaged CFRP's—effects and conclusions for acousto-ultrasonic applications. In: The 7th International Workshop on Structural Health Monitoring, pp. 151–158. DEStech Publications, Lancaster (2009)
24. Sohn, H., Dutta, D., Yang, J.Y., Desimio, M.P., Olson, S.E., Swenson, E.D.: A wavefield imaging technique for delamination detection in composite structures. In: Fifth European Workshop on Structural Health Monitoring, pp. 1335–1340. DEStech Publications, Lancaster (2010)
25. Staszewski, W.J., Lee, B., Mallet, K., Scarpa, F.: Structural health monitoring using scanning laser vibrometry; I. Lamb wave sensing. Smart Mater. Struct. **14**(2), 251–260 (2004)
26. Su, Z., Ye, L.: Identification of damage using Lamb Waves. Springer, Berlin (2009) ISBN: 978-1-84882-783-7
27. Vivar-Perez, J.M., Willberg, C., Gabbert, U.: Simulation of piezoelectric induced Lamb waves in plates. In: PAMM-Proceedings, Applied Mathematics and Mechanics, vol. 9, issue no. 1, pp. 503–504. (2009)
28. von Ende, S., Lammering, R.: Modeling and simulation of Lamb wave generation with piezoelectric plates. Mech. Adv. Mater. Struct. **16**(3), 188–197 (2009)
29. Willberg, C., Vivar-Perez, J.M., Ahmad, Z., Gabbert, U.: Simulation of piezoelectric induced Lamb waves in plates. In: The 7th International workshop on structural health monitoring, pp. 2299–3006. DEStech Publications, Lancaster (2009)
30. Windisch, T., Schwerz, R., Schubert, L, Köhler, B.: Angle-resolved study of Lamb wave generation and experimental investigation of wave attenuation by laser vibrometry. In: Fifth European Workshop on Structural Health Monitoring, pp. 800–805. DEStech Publications, Lancaster (2010)
31. Zak, A., Krawzuk, M., Ostachowicz, W.: Propagation of guided elastic waves in shell-type aircraft structural elements. In: Fifth European Workshop on Structural Health Monitoring, pp. 1031–1038. DEStech Publications, Lancaster (2010)